

We are IntechOpen, the world's leading publisher of Open Access books Built by scientists, for scientists

6,900

Open access books available

186,000

International authors and editors

200M

Downloads

Our authors are among the

154

Countries delivered to

TOP 1%

most cited scientists

12.2%

Contributors from top 500 universities



WEB OF SCIENCE™

Selection of our books indexed in the Book Citation Index
in Web of Science™ Core Collection (BKCI)

Interested in publishing with us?
Contact book.department@intechopen.com

Numbers displayed above are based on latest data collected.
For more information visit www.intechopen.com



Nano-cones Formed on a Surface of Semiconductors by Laser Radiation: Technology, Model and Properties

Artur Medvid'

*Riga Technical University,
Latvia*

1. Introduction

Nowadays, nanostructures are some of the most investigated objects in semiconductor physics, especially Quantum confinement effect (QCE) in quantum dots (QDs) (Alivisatos, 1996), quantum wires (QWs) (Xia et al., 2003) and quantum wells (Fowler et al., 1966). In the case of nano-size structures the energy band diagram of semiconductor changes strongly. This leads to a crucial change of semiconductor properties such as: electrical, due to the change of free charge carrier concentration and electrons' and holes' mobility; optical, such as: absorption coefficient, reflectivity index, radiative recombination efficiency (Emel'yanov et al., 2005); mechanical and heating properties.

The growth of investigations of the homogeneous structures, such as well-defined one-dimensional axial heterostructures, multiheterostructures and core-shell nano-wire heterostructures generates a great interest for their potential applications. Conglomeration of the QDs in a line leads to formation of QWs. If diameter of QWs changes monotonously then cones like structure is formed. The cone nanostructure properties have not only quantitative, but also strongly qualitative characteristics and new interesting properties, for example, formation of graded band gap structure in elementary semiconductors (Medvid' et al., 2008).

Fabrication of nanostructures without lithographic process, based on the self-assembling processes is very promising for future nano-electronics. In this case the self-assembling processes utilize the microscopic structures on the surface or the strain induced by lattice mismatch.

Today we have only some very well elaborated methods for formation of nanostructures (NSs) in semiconductors. They are: molecular beam epitaxy (Talochkin et al., 2005), ion implantation (Zhu et al., 1997) chemical vapor deposition method (Hartmann et al., 2005), and laser ablation (Morales et al., 1998, Yoshida et al., 1998) with followed by thermal annealing in furnace. A lot of time and high vacuum or special environment, for example, inert gas Ar is needed for nano-crystals growth using these methods. As a result, nano-crystals grow with broad distribution in size. Therefore, elaboration of new methods for growth of NSs in semiconductors is a very important task for nano-electronics and optoelectronics. A significant amount of effort has been dedicated to the production of nano-structured Si-based systems (Werva et al., 1996). Several studies have used ion implantation

Source: Nanowires Science and Technology, Book edited by: Nicoleta Lupu,
ISBN 978-953-7619-89-3, pp. 402, February 2010, INTECH, Croatia, downloaded from SCIYO.COM

of group IV elements in SiO_2 and heat treatment to obtain NSs that exhibit photoluminescence (PL). Si is the basic material in microelectronics because it is cheap and its technology is very well developed.

Photoluminescence in IR, red, and blue-violet region of spectra of Si and Ge nano-particles implanted into SiO_2 layer have been found by several scientific groups. Strong PL in the blue-violet region was achieved, with the values of excitation and emission energy being independent of the annealing temperature and consequently of the cluster mean size (Werva et al., 1996; Rebohle et al., 2000). Different explanations of this PL mechanism have been proposed. One part of scientists explain the PL by QCE (Rebohle et al., 2000) in Si and Ge nano-particles, but the second part (Fernandez et al., 2002) – by local Si-O and Ge-O vibration at Si- SiO_2 and Ge SiO_2 - interface. Phonon confinement effect model was developed by Campbell and Fauchet (Campbell et al., 1986) for Si nano-crystals. It was shown that using simultaneously micro-Raman back scattering spectrum and PL spectrum it is possible to determine the origin of the PL. It means if “blue shift” in PL spectrum and “red shift” of LO line in Raman back scattering spectrum are simultaneously present QCE takes place in NSs. A new flexible possibility is predicted to change the semiconductor basics parameters into QDs of $\text{Si}_x\text{Ge}_{1-x}/\text{Si}$ solid solution both by change of x (concentration of Ge) and QDs diameter. Increase both content of Ge atoms – x , and diameter of QDs leads to the same effective shift of PL spectrum toward low energy of spectrum, so called “red shift”. It has been shown that increase of x from 0.096 to 0.52 leads to shift of maximum position in IR part of PL spectrum toward low energy (0.3 eV) (Sun et al., 2005). The same, “red shift” of PL spectrum on 0.7 eV has been observed for nano-particles with diameter 5-50 nm and $x = 0.237 - 0.75$ in visible part of spectrum (Mooney et al., 1995). Authors explain this result by the incorporation of the Ge atoms into Si nano-particles and associate it with surface state. Another effect has been observed for pure i-Ge crystal. Decrease of QDs diameter till 4 nm leads to “blue shift” of PL spectrum with maximum position up to 1.65 eV (Medvid’ et al., 2007) in comparison with PL spectrum of bulk crystal. Therefore in this paper we will show that the main role in control of PL spectrum and its intensity is QCE with small influence of Ge content.

Compound semiconductor crystals such as GaAs, 6H-SiC, CdTe and ternary solid solutions CdZnTe are very useful materials in performance of the semiconductor laser, x and y ray detectors (Gnatyuk et al., 2006) and recently it was found that they can be used for construction of solar cells (Vigil-Galan et al., 2005). New possibility for these devices construction was opened using QCE resulting in, for example, increase of laser radiation intensity and increase of efficiency for the third generation solar cells (Green et al., 2004), construction of light sources with controllable wave length i.e. Therefore, research of possibility of NSs formation on a surface of the semiconductors by laser radiation and study of their optical properties are the main tasks of the study. With this aim it is necessary to know the mechanism of the powerful laser radiation (LR) interaction with a semiconductor. The basic model used today for description of LR effects in semiconductor is the thermal model (Beigelsen et al., 1985), at list for nanosecond laser pulls duration. It implies that energy of light is transformed into thermal energy. But it is only the first step in the understanding of this process. Different models have been proposed for explanation of self-assembly of NSs on a surface of a semiconductor by LR. One of them is photo-thermo-deformation (PTD) model (Emel’janov et al., 1997). According to the PTD model conversion of the light to the heat and deformation of the crystalline lattice of a semiconductor takes place due to inhomogeneous absorption of the light. And formation of the periodical

structure on the surface arises due to redistribution of interstitials and vacancies. Disadvantage of the RTD model are following: impossibility to explain of the NSs formation in semiconductors, for example, Ge (Medvid' et al., 2005) and 6H-SiC (Medvid' et al., 2004) at high intensity of LR when phase transition from solid state to liquid phase takes place, accumulation and saturation effects (Medvid' et al., 2002; Medvid' et al., 1999). It was shown that at high absorption of the powerful LR in a semiconductor high gradient of temperature occurs which causes impurities atoms and intrinsic defects, interstitial and vacancies, drift toward temperature gradient, so called Thermogradient effect (TGE) (Medvid' et al., 1999). According to TGE theory atoms which have bigger effective diameter than atoms of basic semiconductor material drift toward the maximum of temperature, but atoms with smaller effective diameter toward the minimum of temperature. As a result in semiconductor arises compressive mechanical stress on the irradiated surface and tensile mechanical stress in the bulk of a semiconductor. An evidence of the TGE presence at these conditions is formation of p-n junction on a surface of p-Si (Mada et al., 1986), p-InSb (Fujisawa, 1980; Medvid' et al., 2001), p-CdTe (Medvid' et al., 2001) and p-InAs (Kurbatov et al., 1983).

A new laser method elaborated for cone like nanostructure (diameter of the nano-cone is increased gradually from top of cone till a substrate) formation on a surface of semiconductors is reported. Model of the nanostructures formation and their optical properties are proposed.

2. Experiments and discussion

2.1 Experiments on elementary semiconductors Ge, Si their solid solution $\text{Si}_x\text{Ge}_{1-x}$ and compound 6H-SiC single crystals.

Experiments were performed in ambient atmosphere at pressure of 1 atm, $T = 20^\circ\text{C}$, and 60% humidity. Radiation from a pulsed Nd:YAG laser for Ge single crystals and $\text{Si}_x\text{Ge}_{1-x}$ /Si solid solution basic frequency with following parameters: pulse duration $\tau = 15$ ns, wavelength $\lambda = 1.06$ μm , pulse rate 12.5 Hz, power $P = 1.0$ MW and for Si single crystals with SiO_2 cover layer second harmonic with $\tau = 10$ ns and $\lambda = 532$ nm were used. SiO_2 cover layer, in experiments with Si, GaAs and CdZnTe, for private evaporation of material is used. Usually laser beam was directed normally to the irradiated surface of sample. Samples of Ge(111) or Ge(001) i-type single crystal with sizes $1.0 \times 0.5 \times 0.5$ cm^3 and resistivity $\rho = 45$ $\Omega\cdot\text{cm}$ were used in experiments. The samples were polished mechanically and etched in CP-4A solution to ensure the minimum surface recombination velocity $S_{\text{min}} = 100$ cm/s on all the surfaces. The spot of laser beam of 3 mm diameter was scanned over the sample surface by a two coordinate manipulator in 1 or 2 mm steps. N_2 laser with following parameters: $\lambda = 337$ nm, $\tau = 10$ ns and $P = 0.16$ MW in experiments with 6H-SiC (0001) single crystals doped with N and B atoms was used. The surface morphology was studied by atomic force microscope (AFM) and electron scanning microscope and electron scanning microscope (ESM). Optical properties of the irradiated and no irradiated samples were studied by photoluminescence (PL) and back scattering Raman methods. For PL the 488nm line of a He-Cd laser and for micro-Raman backs catering a Ar+ laser with $\lambda = 514.5$ nm were used. The AFM study of Ge surface morphology after irradiation by basic frequency of the Nd:YAG laser is shown in Fig.1

The most interesting results were found at increasing the LR intensity up to 28.0 MW/cm^2 , when nano-cones arise on the irradiated surface of Ge, which are self-organized into a 2D lattice. The 2D picture of the irradiated surface of a Ge sample as seen under ESM is shown

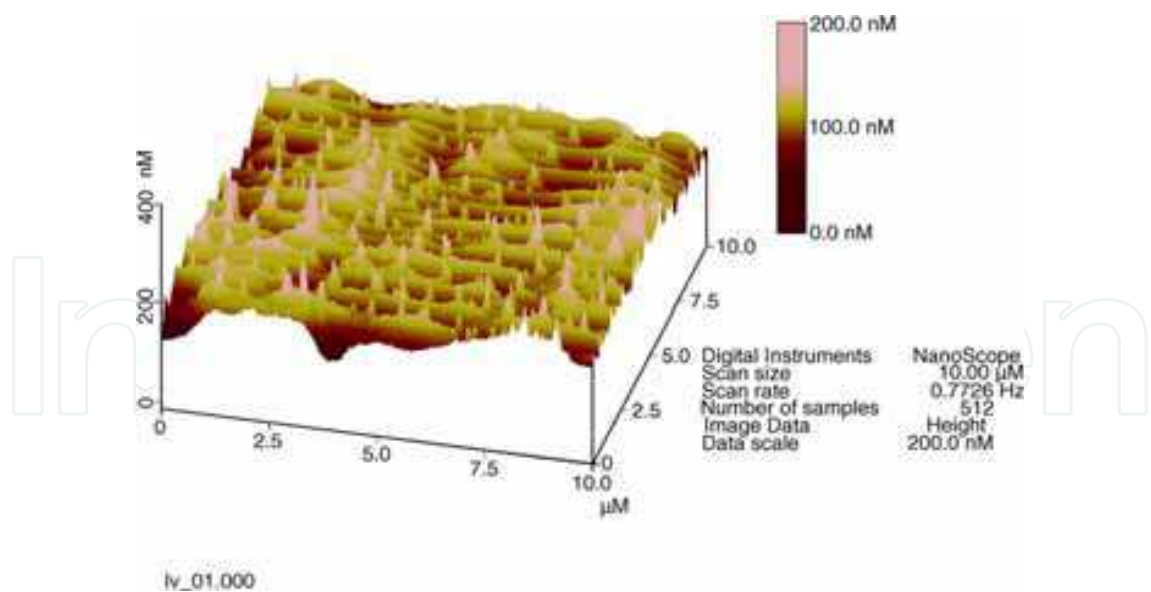


Fig. 1. Three-dimensional AFM image of self-organized nano-structures formed under Nd: YAG laser radiation at intensity of 28 MW/cm².

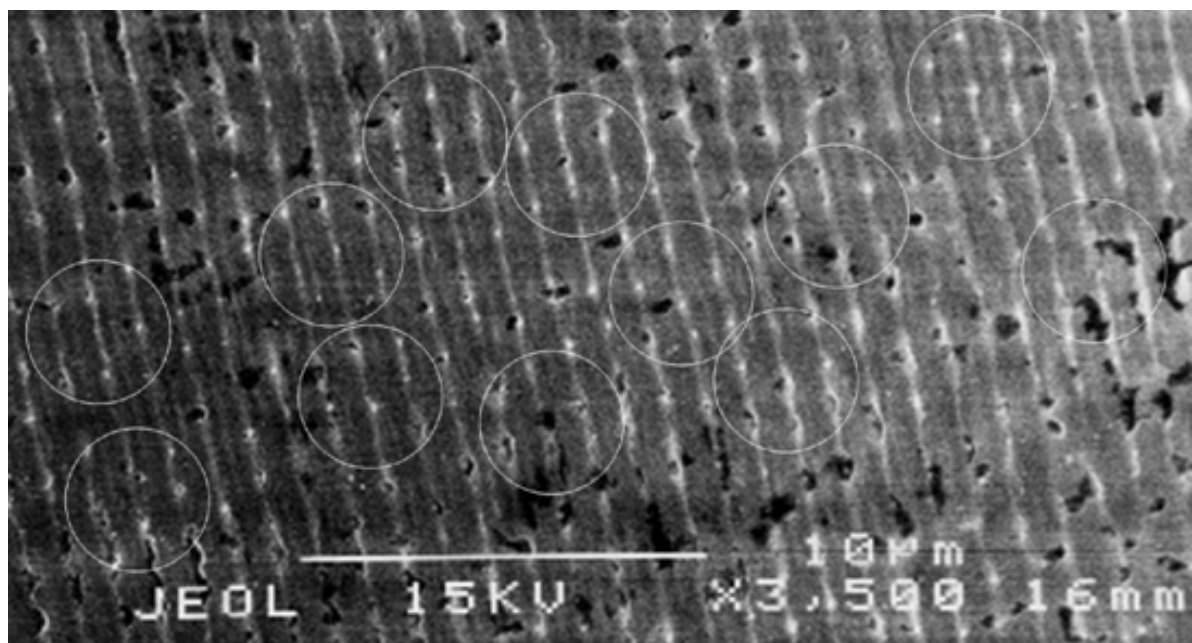


Fig. 2. SEM image of the Ge single crystal surface irradiated by Nd:YAG laser at intensity 28 MW/cm². C_{6i} patterns are marked by white circles.

in Fig. 2. The 2D lattice is characterized by translation symmetry along and perpendicular to periodic lines with a pattern of C point group symmetry and repetition period of 1 μm. C_{6i} patterns are marked by white circles. Patterns orientation and their symmetry depending on orientation of Ge surface were not observed. An explanation of the phenomenon was sought in calculations of the time-dependent distribution of temperature in the bulk of the Ge sample using the heat diffusion equation with values for Ge parameters from (Okhotin et al., 1972; Vorobyev et al., 1996) (Fig. 3). As seen from the results, a close to adiabatic overheating of the crystalline lattice (Lin et al., 1982; Von der Linde et al., 1982) under conditions of the experiment; at LR intensity exceeding 28.0 MW/ cm². A thermal gradient

of $3 \cdot 10^8$ K/m is reached during the first 10 ns. According to synergy ideas, a turbulent fluency and self-organized stationary structures of hexagonal symmetry, the so-called Bernar’s cells, may arise at the presence of non-equilibrium liquid phase at a high gradient of temperature.

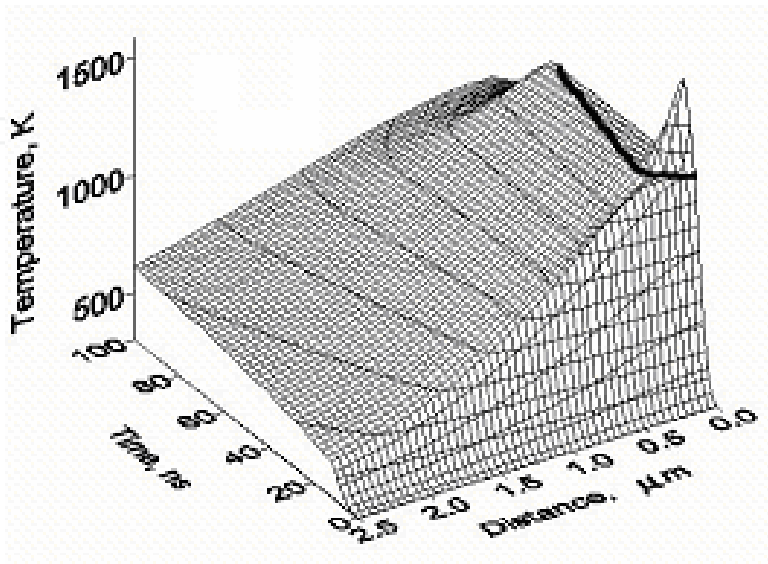


Fig. 3. Calculations of time-dependent distribution of temperature in the bulk of Ge single crystal at Nd:YAG laser radiation intensity of 28 MW/cm². Black line is isotherm of Ge melting temperature.

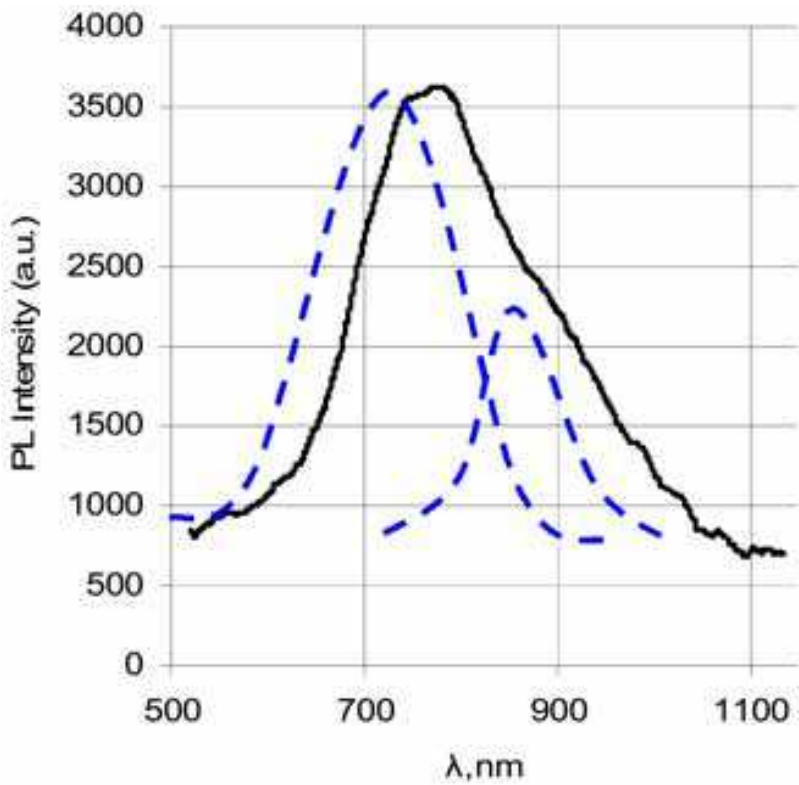


Fig. 4. PL spectrum of the surface of Ge after irradiation by Nd:YAG laser at intensity up to 28 MW/cm².

The characteristic size of the pattern is determined by thickness of the liquid layer being approximately 1 μm in our experiments. Unusual PL spectrum from the irradiated surfaces of Ge was found in the visible range of spectrum with maximum at 750 nm (1.65 eV), as shown in Fig. 4. PL spectrum is usual situated at 2 μm and intensity of PL is very too low due to indirect band structure of Ge. This “blue shift” of PL spectrum we explain by presents of QCF on the top of nano-cones where ball radius is equal or less than Bohr’s radii of electron and hole. Our calculation of the ball diameter on the top of nano-cone using formula (1) from paper (Efors et al., 1982) and band gap shift from PL bands with maximums at 1.65 eV and 1.3 eV (Fowler et al., 1966) at parameters of Ge: $m_e=0.12 m_0$ and $m_h=0.379 m_0$ for electron and hole effective masses, respectively, gives diameters of balls 4 nm and 6 nm.

$$E_g = E_g^0 + \frac{(\pi\hbar)^2}{2d^2} \left(\frac{1}{m_e^*} + \frac{1}{m_h^*} \right) \quad (1)$$

An evidence of our suggestion is Raman back scattering spectra of the no irradiated (black curve) and of the irradiated (red curve) surfaces of Ge crystal by the laser, as shown in Fig.5.

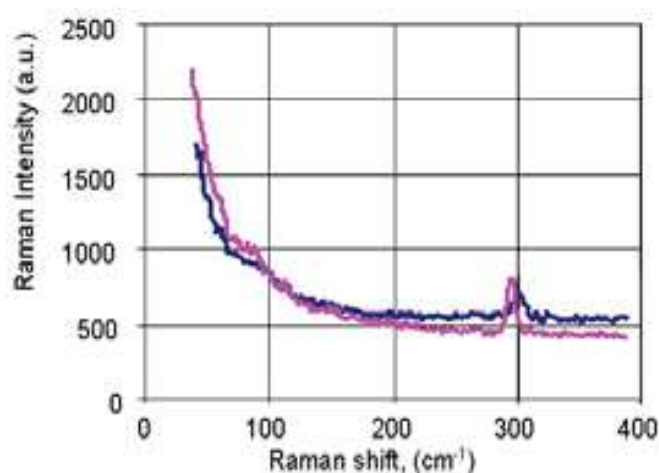


Fig. 5. Micro Raman spectrum of the no irradiated (black curve) and of the irradiated surfaces of Ge single crystal by Nd:YAG laser (red curve) at intensity up to 28 MW/cm².

Line at 300 cm⁻¹ of the no irradiated surface of Ge attributed to bulk Ge (Ge-Ge vibration, LO line). Red shift of the LO line in Raman back scattering spectra on 6 cm⁻¹ after irradiation of Ge surface takes place. Calculated line width and peak frequency Raman spectrum as a function of average crystal size (d_{ave}) for spherical Ge particles from paper (Kartopu et al., 2004) are shown in Fig.6. “Red shift” of the LO line on 6 cm⁻¹ in the Raman spectrum correspond to 4 nm diameter of Ge nano-ball on the top of nano-cone. This value is in good agreement with our previous calculation from formula (1) using the PL spectrum.

An AFM 3D image of Si surface after irradiation by second harmonic of Nd:YAG laser at $I=2.0 \text{ MW/cm}^2$ of SiO₂/Si structure, and the same AFM 3D image of Si surface after subsequent chemical etching by HF are shown in figure 7a and figure 7b, respectively. Photoluminescence spectra of the irradiated (curves 1 and 2) and non-irradiated (curve 3) surface of SiO₂/Si at intensity of laser radiation up to 2.0 MW/cm² are shown in figure 8. The surface morphology of SiO₂ layer is smooth “stone-block” like, but really under SiO₂

layer are very sharp Si nano-cones (Fig. 7b), which arise on the SiO₂/Si interface after irradiation by the laser. SiO₂ layer was fully removed by HF acid from SiO₂/Si structure. Photoluminescence of the SiO₂/Si structure in visible range of spectrum with maximum at 2.05 eV (600 nm) obtained after irradiation by the laser at intensity $I = 2.0 \text{ MW/cm}^2$, is shown in figure 8. PL of this structure after removing of SiO₂ layer by chemical etching in HF acid is similar and is obtained in the same range of spectrum and having the same positions of maximums. It means that PL is not connected with local Si-O vibration at Si-SiO₂ interface (Fernandez et al., 2002). Therefore, we explain our results by Quantum confinement effect in nano-cones. Decrease of the PL intensity can be explained by increase of reflection index of the structure after removing of SiO₂ layer. We can see that the visible PL spectrum of

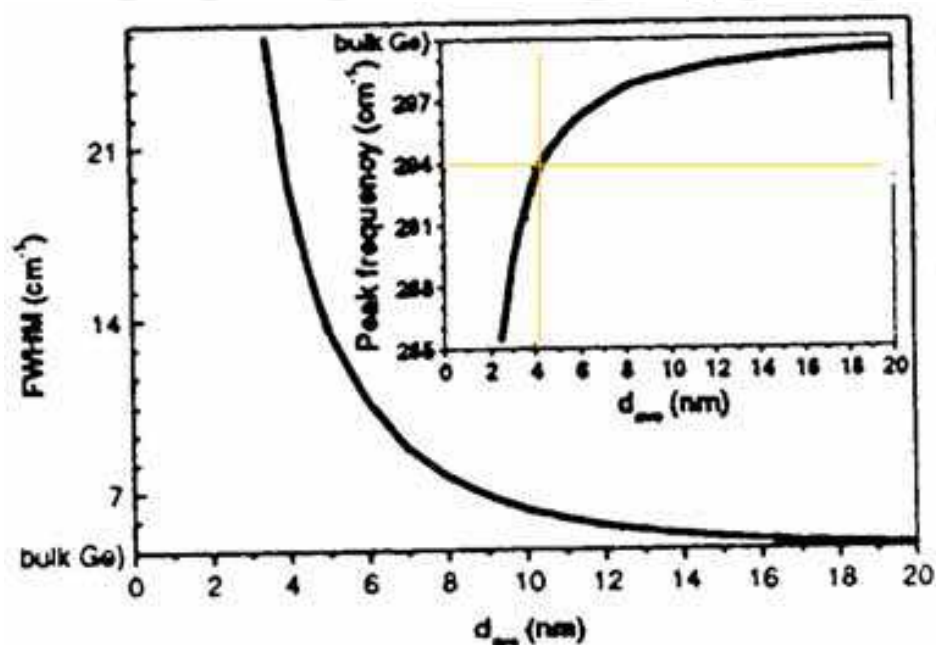


Fig. 6. Calculated line width (FWHM) and peak frequency Raman spectrum as a function of average crystal size (dave) for spherical Ge particles [4].

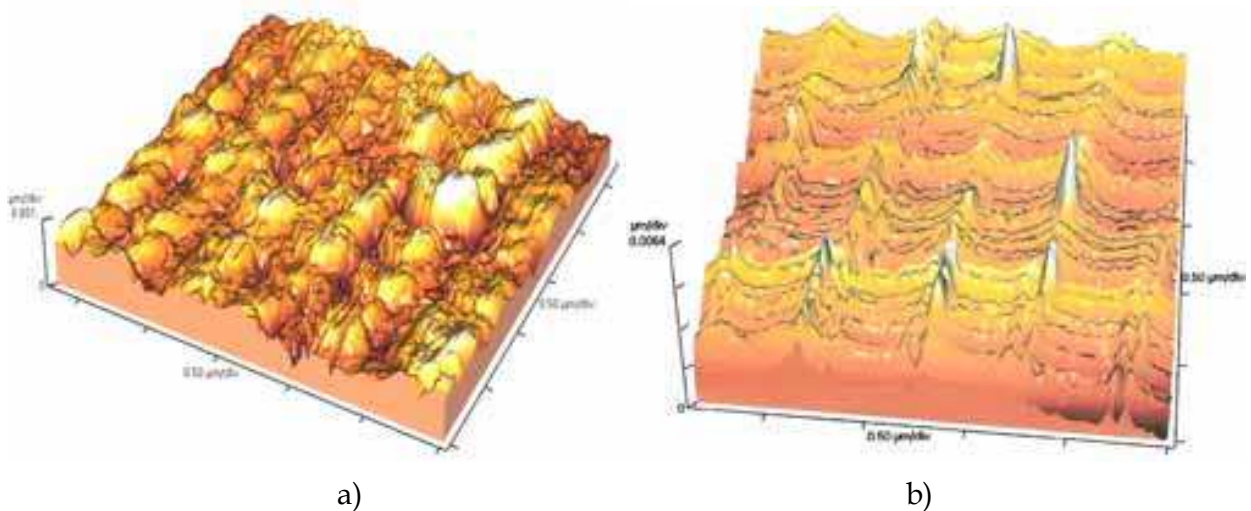


Fig. 7. AFM 3D images of: (a) SiO₂ surface after irradiation of SiO₂/Si structure by Nd:YAG laser at $I = 2.0 \text{ MW/cm}^2$ and (b) Si surface after subsequent removing of SiO₂ by HF acid.

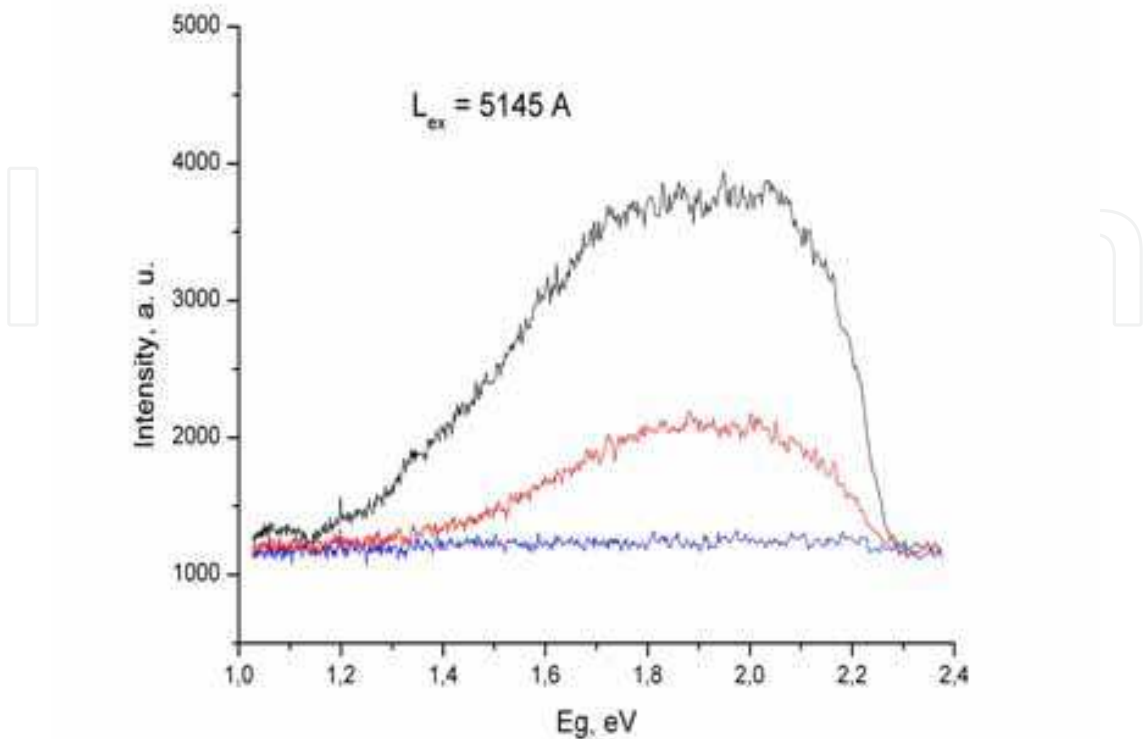


Fig. 8. Photoluminescence spectra of the SiO₂/Si structure irradiated by the laser at intensity 2.0 MW/cm² (red and black curves), after removing of SiO₂ layer by chemical etching in HF acid (black curve). Blue curve correspond to PL of the no irradiated surface.

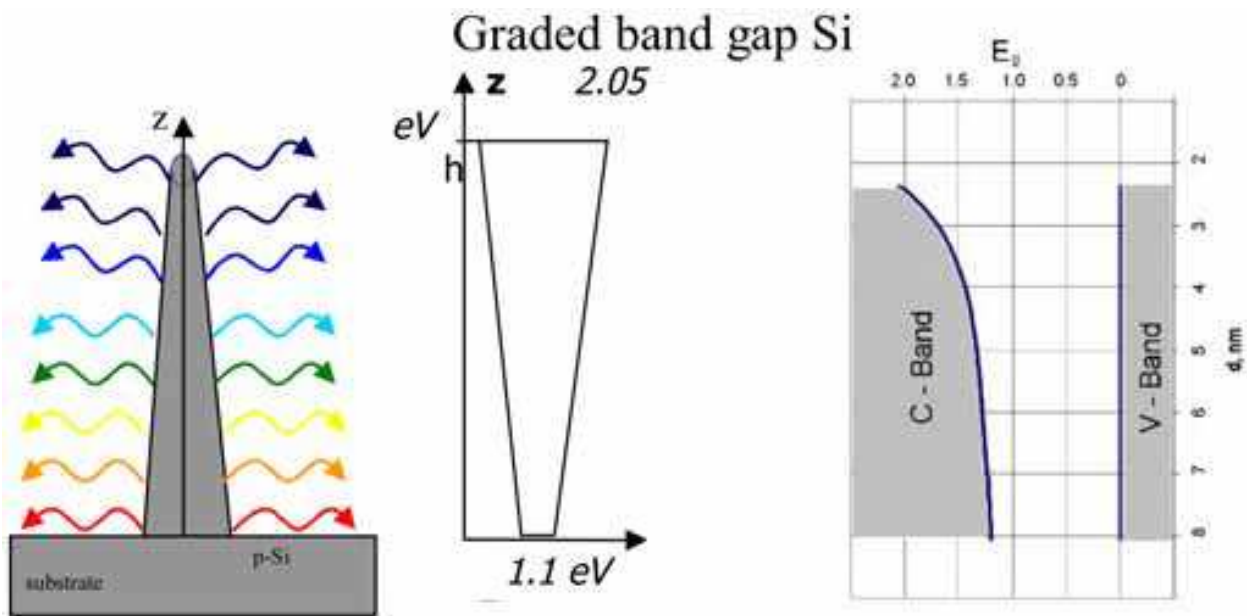


Fig. 9. A schematic image of a nano-hill with a gradually decreasing diameter from p-Si substrate till top, formed by laser radiation - a. and band gap Si structure b. c. A calculated band gap structure of Si as a function of nano-wires diameter using formula (2) from ref. [37].

SiO₂/Si structure is wide and asymmetric with gradual decrease of intensity in IR range of the spectra. It is typical for graded band gap structure. These results present a dramatic rise of PL with energy much higher than the indirect band gap of Si. Schematic image of a nano-cone with graduated decrease of diameter from p-Si substrate till top is shown in Fig.9.

Increase of energy of a radiation quantum from substrate till top of the Si single crystal at photoluminescence of nano-cone takes place due to Quantum confinement effect in nano-wire, according to formula (Li et al., 2004)

$$\Delta E_g = \frac{2\hbar^2 \zeta^2}{m^* d^2}, \quad (2)$$

where $1/(m^*) = 1/(m_e^*) + 1/(m_h^*)$, (m_e^* and m_h^* are electron and hole effective-masses, respectively) and d is the diameter. For QWs, $\zeta = 2.4048$. In our case the diameter of nano-cone/nano-wires is a function of height $d(z)$, therefore, it is graded band gap semiconductor. Our calculation of Si band gap as a function of nano-wires d from PL spectrum using formula (2) from paper (Li et al., 2004) is shown in Fig.9. We can see that the dependence is nonlinear and decreasing function of diameter, especially very rapidly at the small size of diameters. In our case the maximum of band gap is 2.05 eV which corresponds to the minimal diameter 2.3 nm on the top of nano-cones / nano-wire.

We have found a new method for formation of the graded band gap in elementary semiconductor. Graded change of band gap arises due to Quantum confinement effect. Usually graded band gap semiconductor structure is formed by conventional method - molecular beam epitaxy, changing molecular components concentration layer by layer.

Crystal Si_{1-x}Ge_x alloys were grown on Si(100) wafers by Molecular Beam Epitaxy (MBE). Si_{1-x}Ge_x films were grown by MBE on top of a 150 nm thick Si buffer layer on Si. Alloys containing 30% Ge were used in the experiments. The surface of a SiGe/Si structure was irradiated by basic frequency of the Nd:YAG laser. The three-dimensional surface morphology of Si_{1-x}Ge_x/Si hetero-epitaxial structure recorded by AFM measurements after irradiation by the Nd:YAG laser at intensities of 7.0 MW/cm² (a) and 20.0 MW/cm² (b) is shown in Fig. 10.

In Fig. 10(a) are seen the nano-cones of the average height of 11 nm formed by laser radiation at the intensity of 7.0 MW/cm². Similar nano-cones of the average height of 27 nm seen in Fig. 10(b) have been obtained by irradiation intensity of 20 MW/cm². Due to higher irradiation intensity they are more compact in diameter and higher. After irradiation of the SiGe/Si hetero-epitaxial structure by the laser at intensity of 7.0 MW/cm² the surface structure begins to look as spots on un wetting material, for example, it looks like water spots on a glass, Fig.10(c). It means that laser radiation induces segregation of Ge phases at the irradiated surface of the material. This conclusion is in agreement with data from paper [38] where it was shown that Ge phase starts formation at 50% concentration of Ge atoms in SiGe solid solution. According to the TGE (Medvid' et al., 2002), it is supposed that laser radiation initiates the drift of Ge atoms toward the irradiated surface of the hetero-epitaxial structure (Medvid' et al., 2009). PL spectra of the Si_{1-x}Ge_x/Si hetero-epitaxial structures with the maxima at 1.60 -1.72 eV obtained after laser irradiation at intensities of 2.0 MW/cm², 7.0 MW/cm² and 20.0 MW/cm² are shown in Fig. 11. The spectra are unique and unusual for the material, because, depending on Ge concentration, the band gap of SiGe is situated

between 0.67 eV and 1.12 eV (Sun et al., 2005). As seen from Fig. 11, the $\text{Si}_{1-x}\text{Ge}_x$ structure emits light in the visible range of spectrum and the intensity of PL increases with the intensity of irradiation. The maximum of the PL band at 1.70 eV is explained by the QCE (Efors et al., 1982). Position of the observed PL peak compared with the bulk material shows a significant “blue shift”. The maxima of PL spectra of the $\text{Si}_{1-x}\text{Ge}_x/\text{Si}$ hetero-epitaxial structure slightly shift to higher energy when the laser intensity increases from 2.0 MW/cm² to 20.0 MW/cm², which is consistent with the QCE too. Our suggestions, concerning to Ge phase formation, are supported by the back scattering Raman spectra are shown in Fig.12.

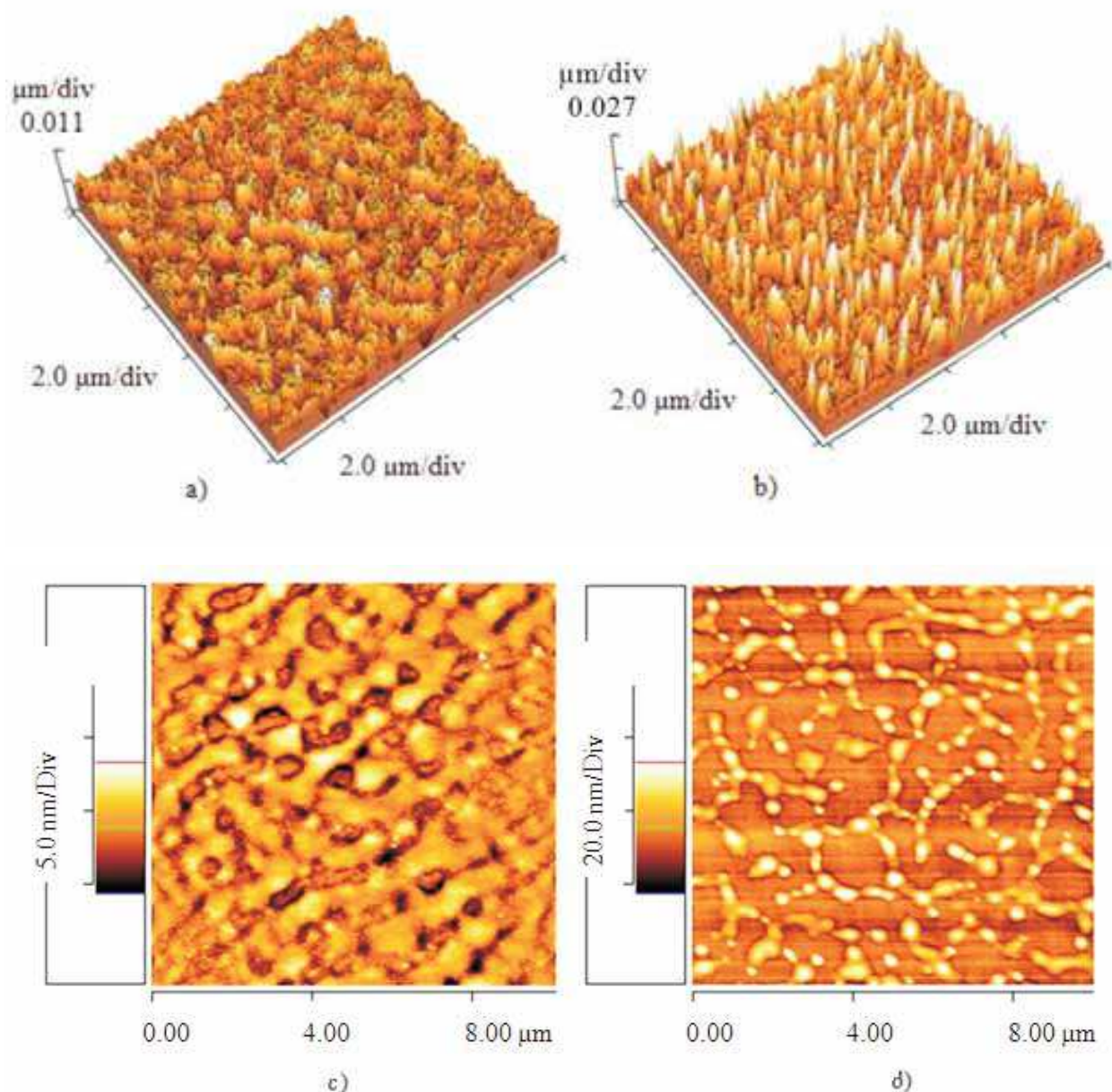


Fig. 10. Three-dimensional AFM images of $\text{Si}_{1-x}\text{Ge}_x/\text{Si}$ surfaces irradiated by the Nd:YAG laser at intensity a) 7 MW/cm² and b) 20 MW/cm² and two-dimensional surface morphology of the same spots of structure at intensities: (c) 7.0 MW/cm² and (d) 20.0 MW/cm².

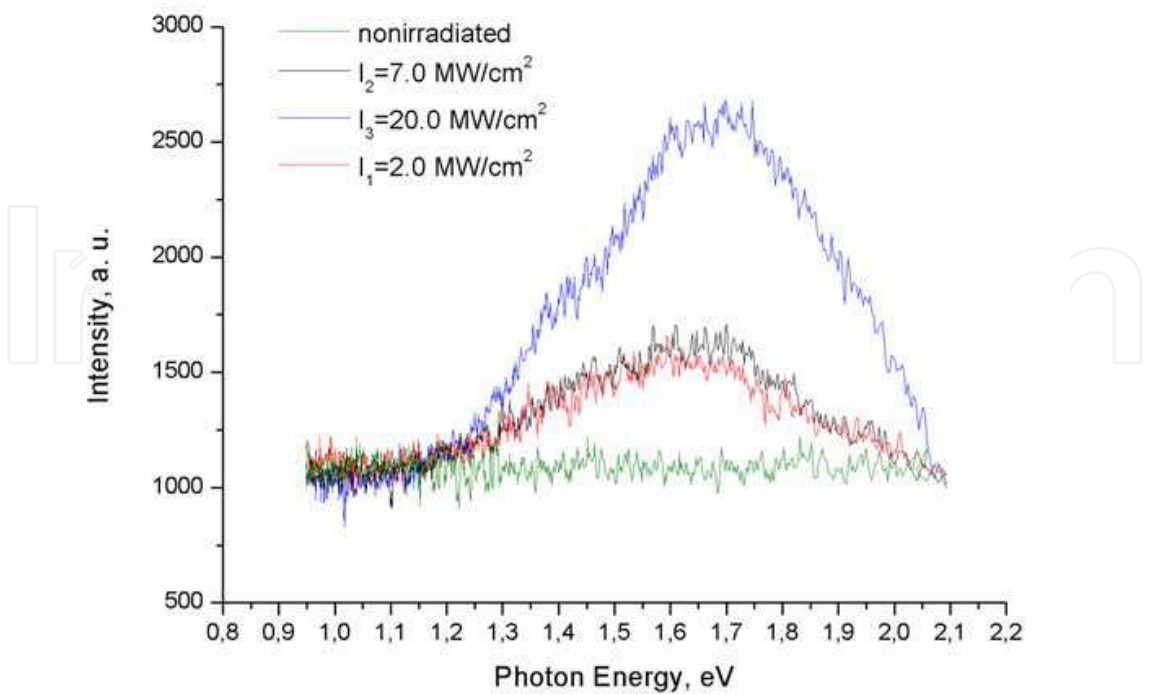


Fig. 11. PL spectra of Si_{0.7}Ge_{0.3}/Si heteroepitaxial structures before and after irradiation by Nd:YAG laser

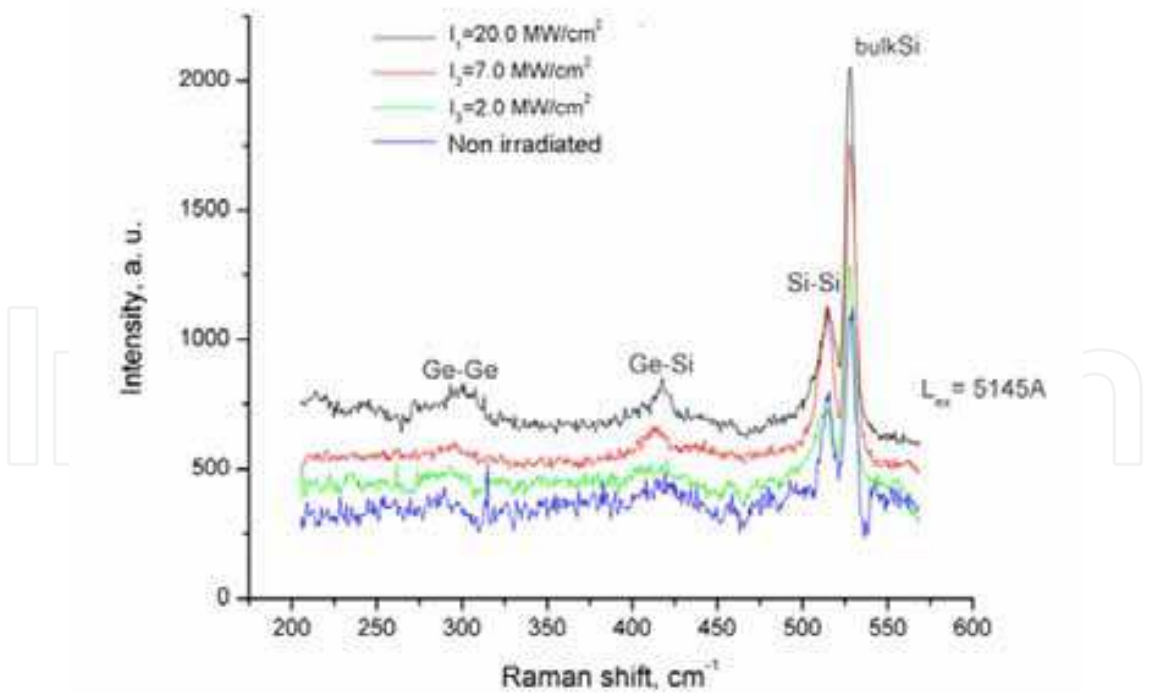


Fig. 12. Back scattering Raman spectra of Si_{1-x}Ge_x/Si heteroepitaxial structure before (blue curve) and after irradiation by the laser. Appearance of the 300cm⁻¹ Ge-Ge vibration band in Raman spectra is explained by the new phase formation in Si_{1-x}Ge_x/Si heteroepitaxial structure.

After laser irradiation at the intensity of 20.0 MW/cm² a Raman band at 300 cm⁻¹ appears in the spectrum. This band is attributed to the Ge-Ge vibration and is explained by formation of a new Ge phase (Kamenev et al., 2005) in the Si_{1-x}Ge_x/Si hetero-epitaxial structure. There is proposed to use modified formula (3) from paper (Efors et al., 1982) for determination of concentration x in the nano-cones of Si_{1-x}Ge_x/Si hetero-epitaxial structure formed by laser radiation using PL spectra.

Determination of x for diameter of nano-dot $d = 4.2$ nm on the top of nano-cone from AFM measurements and band gap from maximums of PL spectra at $E_{g1} = 1.74$ eV, $E_{g2} = 1.69$ eV and $E_{g3} = 1.60$ eV, and $E_g^0 = 0.95$ eV for 30% of Ge in Si (Hogarth, 1965) were found Ge concentration in the nano-cones are $x_1 = 34\%$, $x_2 = 55\%$ and $x_3 = 66\%$, respectively, where E_g^0 is band gap of bulk material, $m_{e,h}^{*Ge,*Si}$ are the electron and hole effective mass for Ge and Si, respectively. In this preliminary analysis we used the same value of d .

$$E_g = E_g^0 + \frac{(\pi\hbar)^2}{2d^2} \left[x_{Ge} \left(\frac{1}{m_e^{*Ge}} + \frac{1}{m_h^{*Ge}} \right) + (1-x)_{Si} \left(\frac{1}{m_e^{*Si}} + \frac{1}{m_h^{*Si}} \right) \right] \quad (3)$$

The following model is proposed for explanation of dynamics of nanostructures formation.

Model

Irradiation of SiGe/Si heterostructure by Nd:YAG laser initiates Ge atoms drift to the irradiated surface due to gradient of temperature - Thermogradient effect. Concentration of Ge atoms is increased at the irradiated surface. Ge atoms are localized at the surface of Si like a thin film. A mismatch of Si and Ge crystal lattices leads to compressed stress of Ge layer. The stress relaxation takes place by plastic deformation of the top Ge layer and creation of nanostructures on the irradiated surface according to the modified Stransky-Krastanov' mode.

In our experiments on SiC the nano-cones is formed on the surface of 6H-SiC after irradiation by the pulsed N₂ laser with following parameters: wavelength 337 nm, pulse duration 10 ns, energy of pulse 1.6·10⁻³ J. These nano-cones are situated along the circular line with diameter about 400 nm as is shown in Fig.13, which is approximately 20 times smaller than the diameter of the spot of the focused laser beam. Usually the focused laser beam forms a crater of a cone shape on the surface of a semiconductor or a metal due to rapid spattering of the melted matter (Kelly et al., 1985). We have used crystals of 6H-SiC, produced by the Lely method doped with N and B or N with following concentrations: $n_N = 2 \cdot 10^{18} \text{cm}^{-3}$ and $n_B = 5 \cdot 10^{18} \text{cm}^{-3}$. The experiments were carried out at room temperature and atmospheric pressure. The PL and the Friction Force Microscope (FFM) were used to detect the laser-induced changes in the chemical composition of the irradiated surface, while the AFM was used for studies of the surface morphology. A C surface of samples was irradiated by the laser. The threshold of average intensity of LR for formation of nanostructures is estimated as $\langle I_{th} \rangle \approx 5 \text{GW/cm}^2$. The FFM studies of the 6H-SiC(N) samples have shown that the chemical composition of nano-cones, which had arisen after the laser irradiation, differs from that of the no irradiated surface.

Luminescence spectra of the laser irradiated and no irradiated 6H-SiC(N) samples are shown in Fig.14, curves 3 and 4, correspondingly. Arising of the 2.8 eV band after laser irradiation is observed. As it is known this luminescence is assigned to the N_C centres (a N atom substituting for C in the lattice) (Gorban' et al., 2001). The observed phenomenon speaks in favor of increase of the nitrogen concentration in laser irradiated surface including the nano-cones.

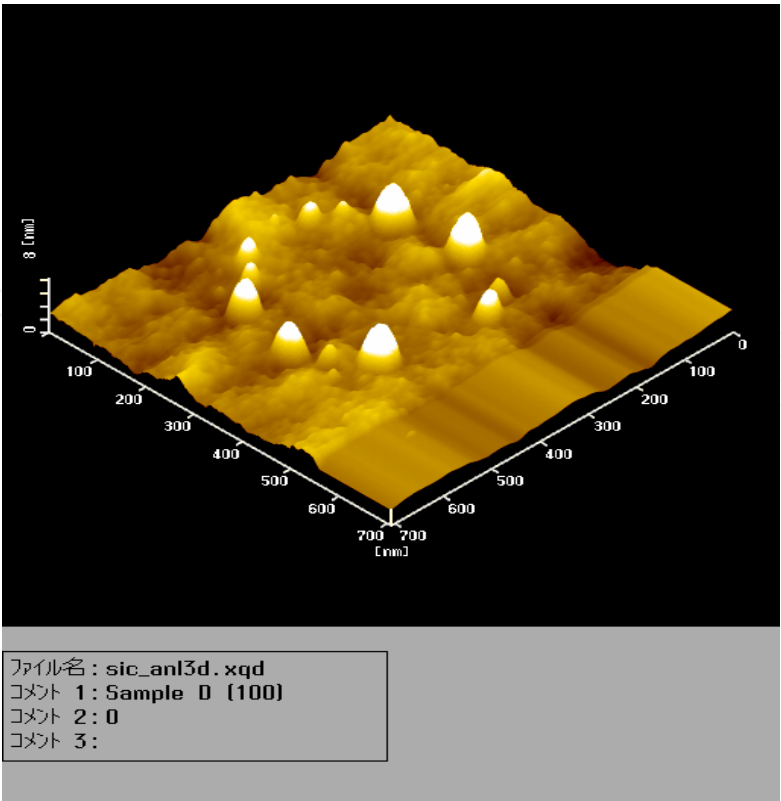


Fig. 13. Morphology of the 6H-SiC(N,B) the C surface after irradiation by N₂ laser at average intensity 5 GW/cm².

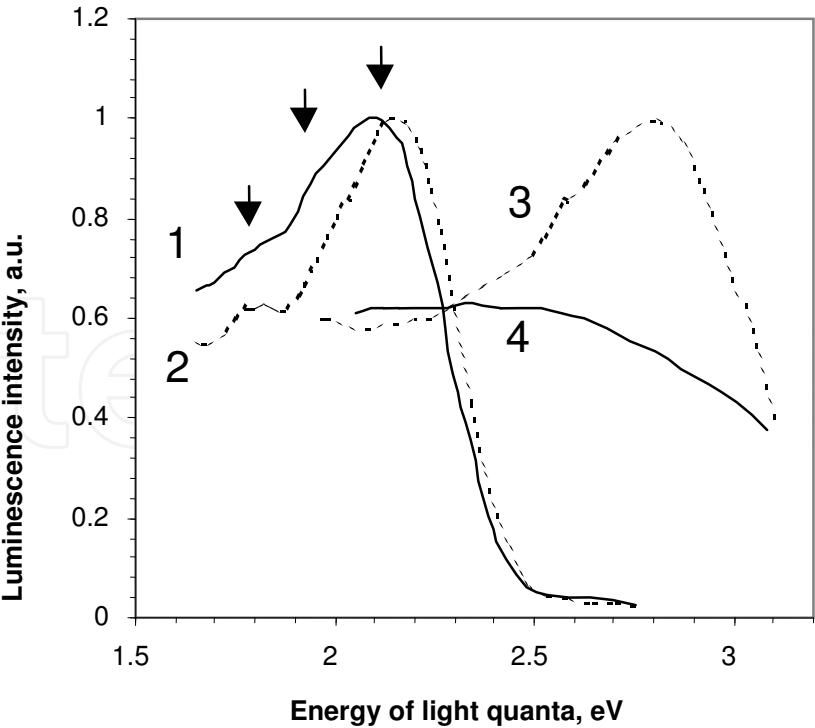


Fig. 14. Spectral distribution of photoluminescence of 6H-SiC samples: curves 1, 2 with impurities N, B and curves 3, 4 with impurity N; solid curves – no irradiated surface, dashed curves - after irradiation by N₂ laser at average intensity up to 5 GW/cm².

The simultaneous formation of nano-cones with the changed chemical composition together with the emergence of the 2.8 eV luminescence band, ascribed to N_C centres allows us to suppose that these luminescence centers could be mainly located in the nano-cones. Consequently, it allows us to propose that the luminescence from the nano-cones is much more intensive than that of the total surface of the sample. Therefore, light emission from the nano-cones could be very bright. Normalized spectra of photoluminescence from non-irradiated and laser irradiated 6H-SiC(N, B) sample are shown at Fig.14, curves 1 and 2, correspondingly. As it is seen from this picture the exposure of the surface of the sample to LR causes the decrease of both the 1.9 eV band, which is known to be originated by the recombination of charge carriers in donor-acceptor (D-A) pairs and 1.78 eV band (of the unknown origin) in comparison with the 2.1 eV band corresponding to electron transition from the conduction band to the boron acceptor level ($E_B = 0.65$ eV) [42]. "Blue shift of PL spectrum and its maximum on 120 meV after irradiation of the sample by N_2 laser at intensity up to 5 MW/cm^2 take place, as can be seen in Fig.14. This effect is explained by QCE on the top of nano-cones.

The threshold character of the effect together with the necessary condition for the energy of the laser light quantum $h\nu > E_g$ (where the E_g is a band gap) for appearance of nano-cones, as well as the increase of N band on PL spectra and the decrease of D-A band of PL under numerous irradiation pulses (80-100 pulses at a point) allow us to suppose the presence of the TGE in these conditions (Medvid' et al., 2002). The TGE leads to redistribution of impurity atoms, vacancies (V) and interstitials as a result of their motion in the temperature gradient field of the crystalline lattice. According to the TGE in the case of SiC(N) the atoms of nitrogen are shifted towards the irradiated surface of the sample, because their covalent radii are larger than that of carbon atom. Due to their motion the N atoms fill the carbon vacancies V_C , resulting in the rise of the 2.8 eV luminescence band. In the SiC(N, B) crystals atoms of boron are shifted towards the opposite direction, because the radius of boron atom is smaller, than that of carbon. As a result, D-A pairs are disarranged and the 1.9 eV luminescence band decreases. We explain the appearance of nano-cones on the surface of 6H-SiC under exposure of a focused N_2 laser radiation by the so-called «lid effect».

"Lid effect" model

The subsurface area of the 6H-SiC crystal could melt in the region of the I_{\max} of LR (Fig.15) because the temperature of the surface is lower than that in the bulk material. Such distribution of the temperature is caused by the low sublimation energy for SiC. The pressure of light is distributed along the surface according to the Gauss function, in Fig.15 dashed curve, and the average pressure is $\langle P \rangle = 1.5$ atm. The pressure of liquid phase is balanced by the pressure of light only in the area of I_{\max} . Beyond this area liquid matter is extruded on the surface in the form of nano-cones presumably along dislocations.

XOY cross-section of the semiconductor on the focused spot of the laser beam is shown together with the distribution of the laser beam intensity I along X coordinate-dashed curve. The dark areas on the surface of the semiconductor are nano-hills and the big dark ring is liquid matter. The black arrows show the pressure of light and the light arrows - the pressure of liquid matter. $\langle P \rangle = 1.5$ atm is average pressure of light.

An evidence of the presence of the "lid effect" in these conditions can be gained from temperature distribution in the depth of the SiC crystal at irradiation by N_2 laser with intensity $I = 4 \cdot 10^8$ W/cm², which is shown in Fig.16. As shown in Fig.16, maximum of temperature is situated in the bulk of the SiC crystal. This black line is isotherm of the melting temperature.

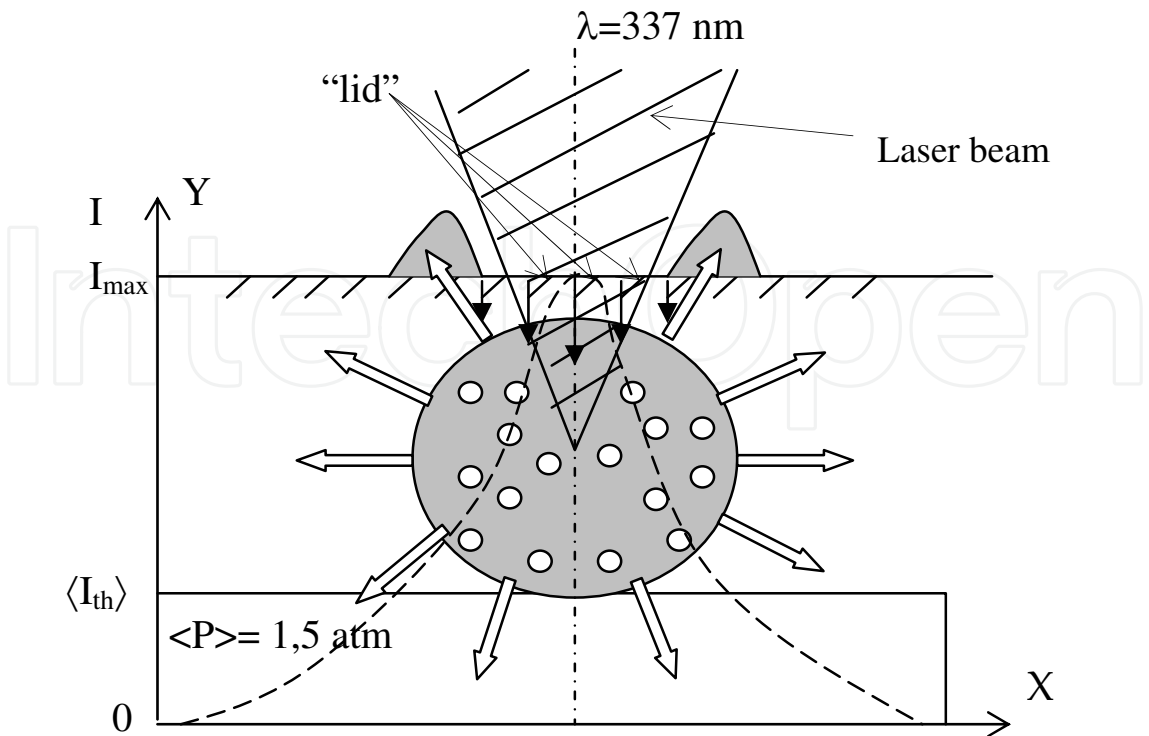


Fig. 15. Scheme of physical model for nano-hills formation on a surface of 6H-SiC caused by N₂ laser radiation $\lambda=337 \text{ nm}$.

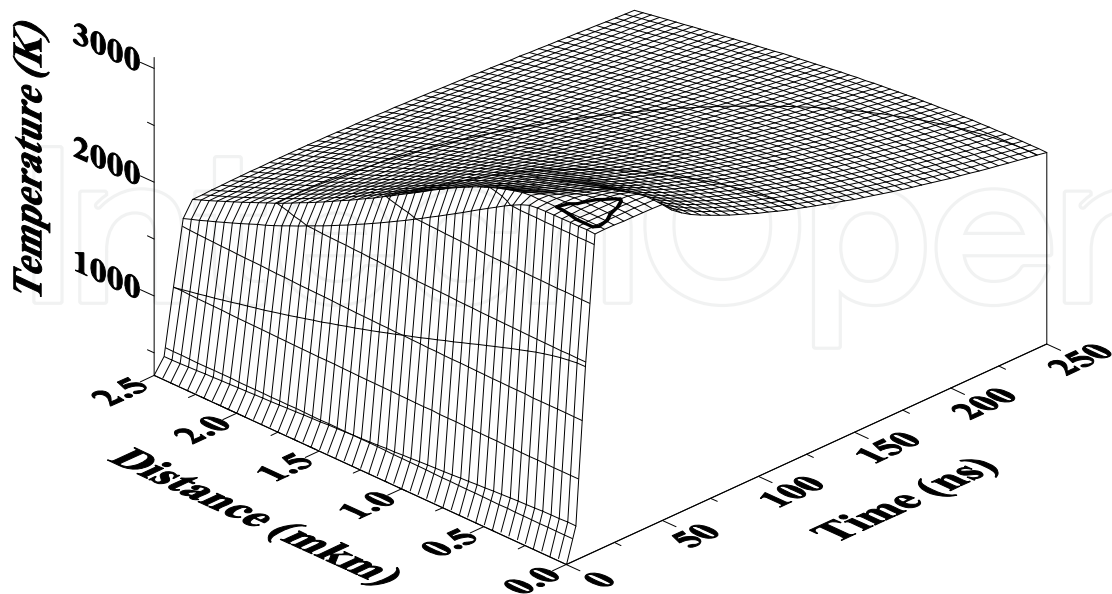


Fig. 16. The calculated distribution of temperature in the depth of SiC crystal after radiation by N laser at intensity $I=0.4 \text{ GW/cm}^2$.

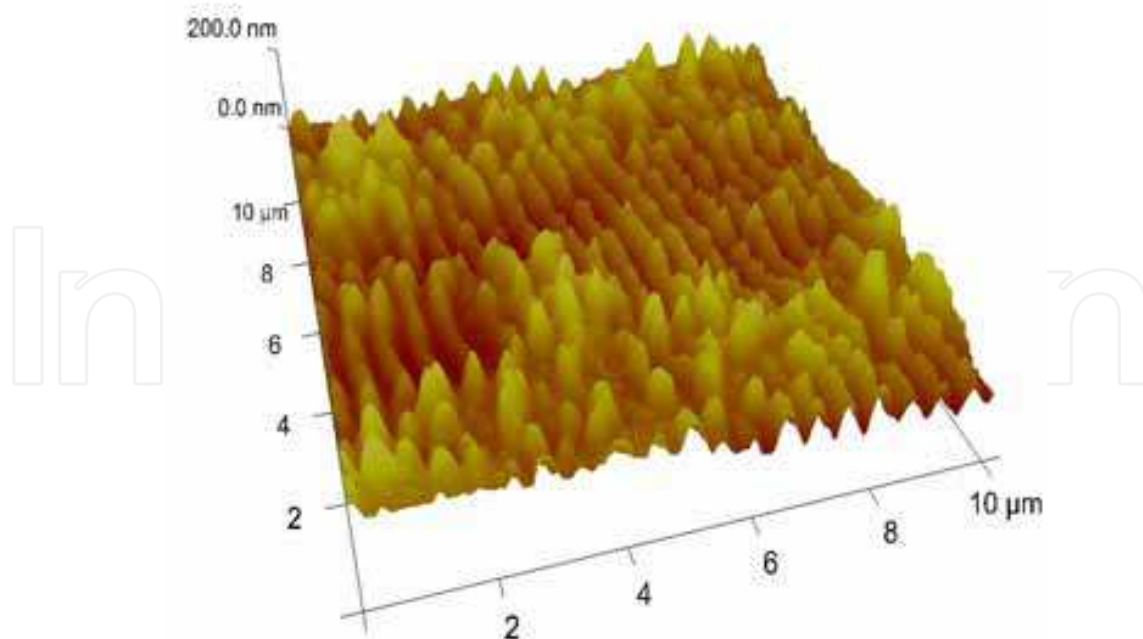


Fig. 17. AFM 3D image of GaAs surface after irradiation by YAG:Nd laser at $I=5.5 \text{ MW/cm}^2$.

2.2 Experiments on binary GaAs and ternary $\text{Cd}_{1-x}\text{Zn}_x\text{Te}$ compound semiconductors

The same methods for study nano-cones on a surface of binary compound GaAs and ternary compound $\text{Cd}_{1-x}\text{Zn}_x\text{Te}$ semiconductors were studied. Nano- The increase of exciton energy on 2.5 meV proves the presence of the exciton quantum confinement effect at the top of nano-hills. The energy of band gap of the $\text{Cd}_{1-x}\text{Zn}_x\text{Te}$ crystal increases along the axis of the nano-hill perpendicular to the sample surface. Thus, a graded band gap structure with optical window is formed in the nano-hill ere formed on the surface of GaAs and $\text{Cd}_{1-x}\text{Zn}_x\text{Te}$ with $x = 0.1$ by the second harmonics of Nd:YAG laser radiation at intensity within $4.0 - 12.0 \text{ MW/cm}^2$.

Morphology of the irradiated surface of the GaAs single crystal has shown formation of very sharp self-organized nano-cones, as shown in Fig. 17, which arise on the irradiated surface after irradiation by the laser with intensity $I = 5.5 \text{ MW/cm}^2$. In the PL spectrum of irradiated GaAs single crystals (Fig.18) with maximum of spectrum at 750 nm we have also observed band gap blue shift on 100 nm. Intensity of PL at the maximum of the irradiated surface is 4 times more that intensity of PL no irradiated surface. But its intensity is much lower comparing to PL of Ge quasi QDs. The evidence of QCE presence in nanostructures on the irradiated surface of GaAs single crystal is back scattering Raman spectra, as shown in Fig. 19. We can see that spectral LO phonon line at 292 cm^{-1} is characterized by “red shift” after irradiation of the surface by the laser. Calculations of quasi quantum dots diameter on the top of nano-cones using band gap shift from PL spectra of GaAs and formula (1) gives $d = 11 \text{ nm}$.

Irradiation of $\text{Cd}_{1-x}\text{Zn}_x\text{Te}$ ($x=0.1$) crystals by the Nd:YAG laser radiation at intensities below the threshold intensity of 4 MW/cm^2 does not change the surface morphology(Fig.20,a). The nanostructures begin forming at intensities $I \geq 4 \text{ MW/cm}^2$ on the irradiated surface, as are shown in Fig.20.a and b, correspondently (Medvid' et al., 2008).

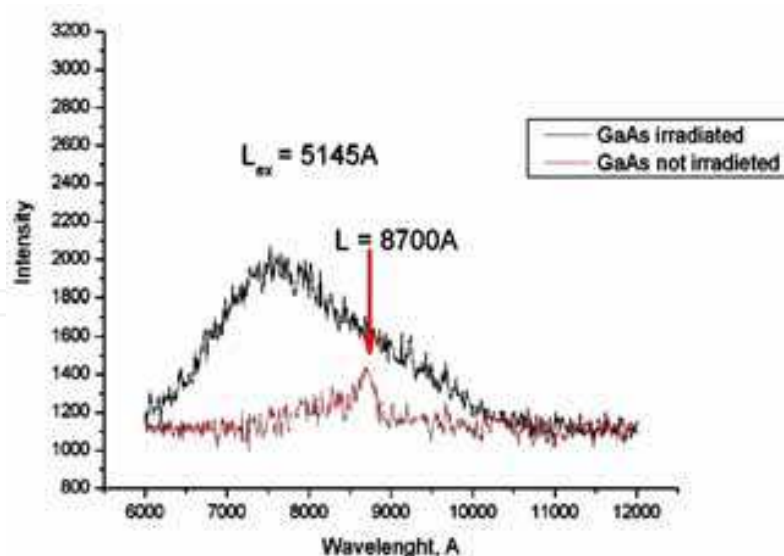


Fig. 18. PL spectra of the irradiated and nonirradiated surface of Si at intensity of LR up to 7.5 MW/cm^2 .

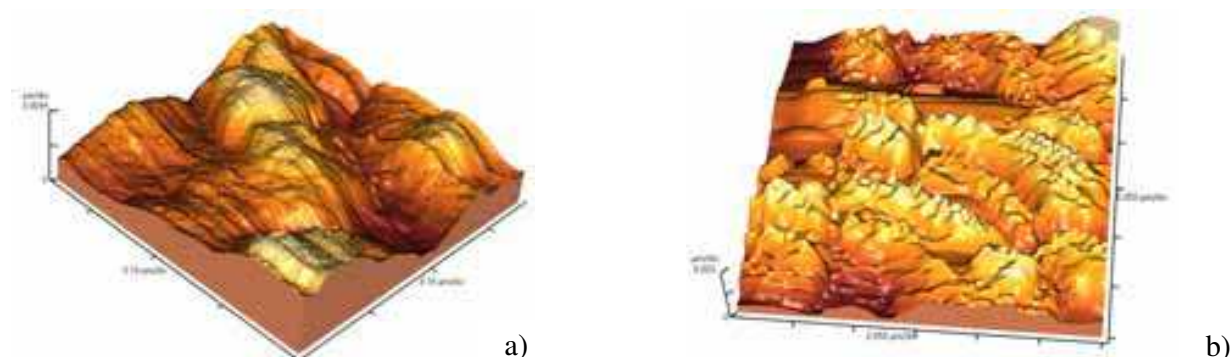


Fig. 20. Atomic force images of the $\text{Cd}_{1-x}\text{Zn}_x\text{Te}$ ($x=0.1$) surface (a) before irradiation and (b) after irradiation by the laser at intensity of 12 MW/cm^2 .

The “blue shift” of exciton bands in PL spectra of the irradiated $\text{Cd}_{1-x}\text{Zn}_x\text{Te}$ is explained by Exciton quantum confinement effect in nano-cones (Brus, 1984). A new PL band at 1.88 eV is found. Appearance of the PL band is explained by formation of $\text{CdTe/Cd}_{1-x}\text{Zn}_x\text{Te}$ heterostructure in the bulk of the semiconductor with $x = 0.7$ due to TGE (Medvid’ et al., 2002). The increase of exciton energy on 2.5 meV proves the presence of the Exciton quantum confinement effect at the top of nano-cones. The energy of band gap of the $\text{Cd}_{1-x}\text{Zn}_x\text{Te}$ crystal increases along the axis of the nano-cone perpendicular to the sample surface. Thus, a graded band gap structure with optical window is formed in the nano-cone. The energy of band gap of the $\text{Cd}_{1-x}\text{Zn}_x\text{Te}$ crystal increases along the ZO axis of the nano-cone perpendicular to the irradiated surface of the sample, as is shown in Fig 22. Thus, a graded band gap structure with optical window is formed in the nano-cone.

The Thermogradient effect plays the main role in the redistribution of Cd and Zn atoms at the irradiated surface of $\text{Cd}_{1-x}\text{Zn}_x\text{Te}$ at low intensities of LR from 0.2 MW/cm^2 till 4.0 MW/cm^2 . Two layers are formed near the irradiated surface of semiconductor: the top layer consists of mostly CdTe crystal but the underlying layer – ZnTe crystal, as is shown in Fig.22.a. A mismatch of lattices of CdTe and ZnTe crystals is equal up to 5.8% . This

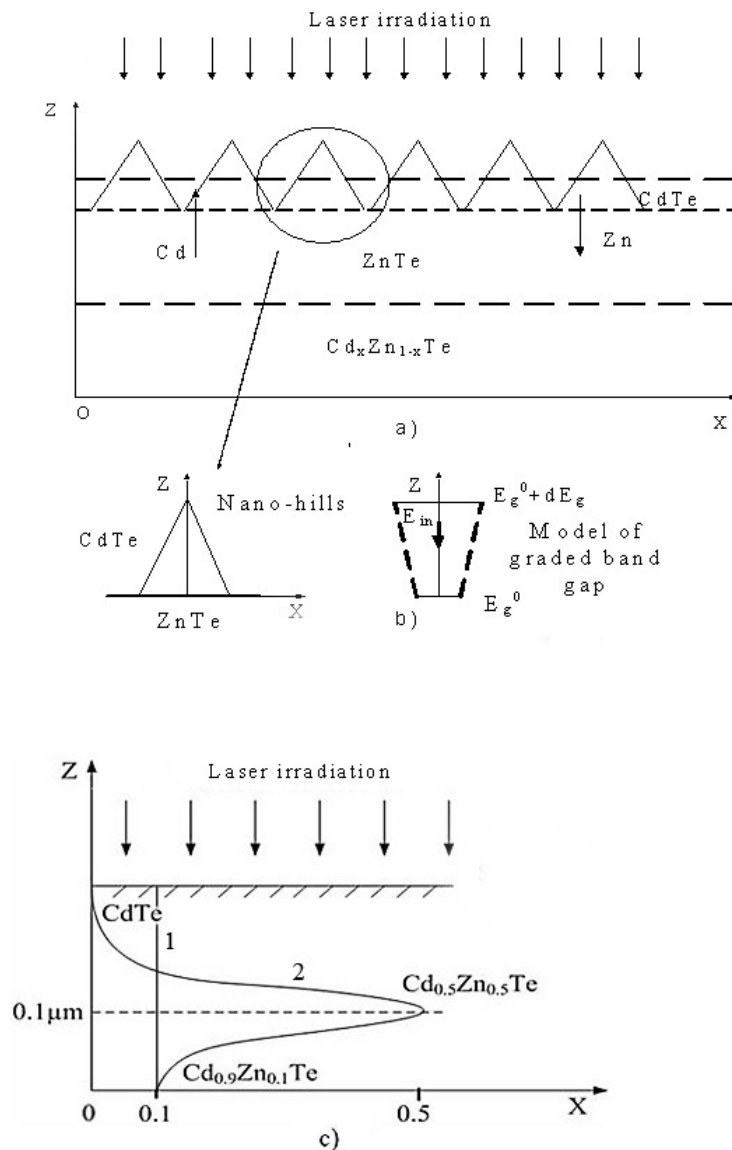


Fig. 22. a) Scheme of physical model for nano-cones formation on a surface of $Cd_{1-x}Zn_xTe$ crystal caused by Nd:YAG laser radiation $\lambda=532$ nm, the laser beam direction, Cd and Zn atoms drift in gradient T field and cross-section of the irradiated sample; b) The energy of band gap of the $Cd_{1-x}Zn_xTe$ crystal increases along the symmetry axis Z of the nano-cone perpendicular to the irradiated surface of the sample. Thus, a graded band gap structure with optical window is formed in the nano-cone due to QCE; c) Distribution of Zn and Cd atoms in Z direction in the sample before (curve 1) and after irradiation by the laser (curve 2).

plastically deformation of the top layer leads to creation of nanostructures of the irradiated surface according to the modified Stransky-Krastanov' mode. This result is in a good agreement with PL measurement data, as shown in Fig. 21.b. A built-in quasi electric field, generated by graded band gap, is directed in the bulk of the semiconductor as a result decrease of surface recombination velocity. The photoconductivity spectra of CdZnTe samples were recorded at room temperature before and after irradiation by Nd:YAG laser, as shown in Fig. 23. The photoconductivity spectra show, that at laser intensity up to $4MW/cm^2$ the shift of maximum spectrum to the longer wavelength, "red shift", of spectra

and increase of photocurrent at short wavelength take place, as shown in Fig.23, green curve. This effect is explained by decrease of surface recombination velocity. The irradiation of the sample by higher intensity of the laser causes the “red shift” of spectra and the total increase of photocurrent up to 2 times, as shown in Fig.23, red and black curves, are explained by formation of graded band gap structure on the top of nano-cones and increase of electron-hole pairs life time due to increase concentration of D-A pairs after irradiation by the laser.

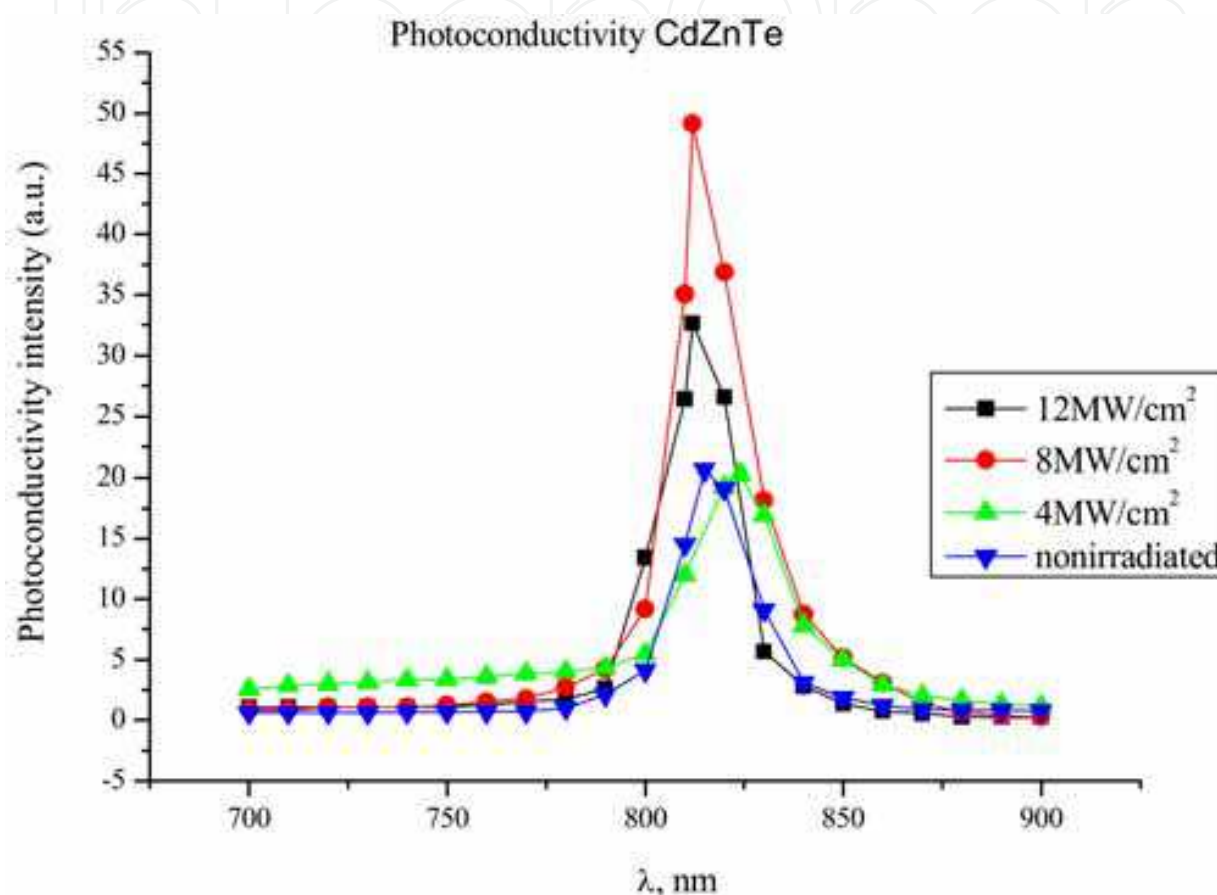


Fig. 23. Photoconductivity spectra of the irradiated surface of $\text{Cd}_{1-x}\text{Zn}_x\text{Te}$ before and after irradiation by the laser.

3. Conclusion

For the first time was shown the possibility of graded band gap structure formation in elementary semiconductors due to the presence of Quantum confinement effect in cone-like nanostructure.

Thermogradient effect plays a main role in initial stage of nano-cones and graded band gap structure formation by laser radiation in semiconductors.

The new laser method for nano-cones formation on a surface of semiconductors Si, Ge, GaAs, 6H-SiC crystals, SiGe and CdZnTe solid solutions is elaborated.

The model of cone-like nanostructure formation on the SiGe surface has been proposed. According to this model, irradiation the semiconductor by strongly absorbed laser radiation, leads to a huge temperature gradient (10^8K/m). It causes the drift of Ge atoms towards the

irradiated surface. Concentration of Ge atoms is increased at the irradiated surface. Ge atoms are localized at the surface of Si like a thin film. A mismatch of Si and Ge crystal lattices leads to compressed stress of Ge layer. The stress relaxation by plastic deformation of the top Ge layer and creation of nanostructures on the irradiated surface according to the modified Stransky-Krastanov' mode takes place.

4. Acknowledgements

The author gratefully acknowledges financial support in part by Europe Project in the framework FR7-218000 Nr. L7477, by the Latvian Council of Science according to the Grant No. L7306, L7455 and by the Riga Technical University projects: FLPP-2009/32, R7355, R7234, U6968 & U7094.

5. References

- Alivisatos, A. P. (1996). Semiconductor Clusters, Nanocrystals, and Quantum Dots. *Science*, Vol. 271, pp.933-937, ISSN: 0036-8075;
- Beigelsen, D.K., Rozgonyi G.A., Shank, C.V. (1985). *Energy Beam-Solid Interactions and Transient Thermal Processing*, Vol.5, Material Research Society, Pittsburgh;
- Brus, L.E. (1984). Electron-electron and electron-hole interactions in small semiconductor crystallites: The size dependence of the lowest excited electronic state, *J.Chem.Phys.*, Vol. 80, No.9, pp.4403- 44, ISSN:0021-9606 ;
- Campbell, H. & Fauchet P.M. (1986). The effects of microcrystal size and shape on the one phonon Raman spectra of crystalline semiconductors, *Solid State Commun.*, Vol.58 pp.739-74, ISSN:0038-1098;
- Efors, A.L. & Efors, A.L. (1982). Band-band absorption of light in semiconductor ball. *Phys. and Techn.of Semicond.*, Vol.16, pp. 1209-121 ;
- Emel'janov, V.I. & Panin, I.M. (1997). Defect-deformational self-organization and nanostructuring of solid surfaces, *Solid State Physics*, Vol.39, pp.2029-2035, ISSN:0081-1947;
- Emel'yanov, A.M. Sobolev, N.A., Mel'nikova, T.M., Abrosimov, N.V. (2005). Point and extended defects engineering, *Solid state phenomena*, Vol.108-109, pp.761-764;
- Fernandez, B.G., Lopez, M., Garcia, C., Perez-Rodriguez, A., Morante J.R., Bonafos, C., Carrada, M.& Claverie, A. (2002). *J.Appl.Phys.* Vol.91 pp. 789-7, ISSN:0021-8979;
- Fowler, A. B., Fang, F. F., Howard, W. E. & Stiles P. J. (1966). Magneto-Oscillatory Conductance in Silicon Surfaces, *Phys. Rev. Lett.*, Vol.16, pp.901-903, ISSN:0031-9007;
- Fujisawa, I. (1980). Type Conversion of InSb from p to n by Ion bombardment and laser Irradiation. *Jpn J. Appl. Phys.*, Vol. 19, pp. 2137-2140, ISSN:0021-4922;
- Gnatyuk, V.A., Aoki, T., Hatanaka, Y. & Vlasenko O.I. (2006). Defect formation in CdTe during laser-induced doping and application to the manufacturing nuclear radiation detectors, *Phys. stat. sol. (c)* Vol.1, pp.121-12, ISSN: 1610-1634;
- Gorban', I.S. & Krokhmal', A.P. (2001). The impurity optical absorption and conduction band structure in 6H-Si. *Semicond.*, Vol.35, pp.1242-1248, ISSN: 1063-7826;

- Green, Martin A. (2004). *Third generation photovoltaics: advanced solar emerge conversion*, Springer-Verlag, Berlin;
- Hartmann, J.M., Bertin, F., Rolland, G., Semeria, M.N. & Bremond, G. (2005). Effects of the temperature and of the amount of Ge on the morphology of Ge islands grown by reduced pressure-chemical vapor deposition, *Thin Solid Films*, Nr. 479, pp.113-120, ISSN: 0040-6090;
- Kamenev, B.V., Baribeau, J.-M., Lockwood, D.J., & Tsybekov, A. (2005). Optical properties of Stranski-Krastanov grown three-dimensional Si/Si Ge nanostructures, *Physica E*, Vol. 26, pp. 174- 17, ISSN:1386-9477;
- Kartopu, G., Bayliss S.C., Hummel, R.E.& Ekinci, Y. (2004). Report on the origin of the orange PL emission band. *J.Appl.Phys.*,Vol.957, pp. 2466-2472 , ISSN: 0021-8979.
- Kelly, R., Cuomo, J.J., Leary, P.A., Rothenberg, J., Rraren, B.E.& Aliotta, C.F. (1985). Laser sputtering Part I: On the eksistence of rapid laser sputtering at 193 nm. *Nuclear Inst. and Meth. in Phys. Research*, Vol.B9, pp.329-340; ISSN: 0168-583x
- Kurbatov, L., Stojanova I., Trohimchuk,P.P.&Trohin,A.S. (1983), Laser anieleing of A^{III}B^V compound. *Rep.Acad.Sc.USSR*, Vol.268, pp.594- 597, (in Russian);
- Kuwabara, H. & Yamada, S. (1975). Free-to-bound transition in β -SiC doped with boron. *Phys. Stat. Sol.(a)*, Vol.30, pp.739-74, ISSN:0031-8965;
- Lin, J.M., Kurz, H.& Blomborgen, N. (1982). Picosecond time-resolved plasma and temperature-induced changes of reflectivity and transmission in silicon. *Appl. Phys. Lett.* , Vol.41, pp.643-64, ISSN:0003-6951;
- Li, J. & Lin-Wang, (2004). Comparison between quantum confinement effects of quantum wires and quantum dots. *Chem.Mater.*, Vol.16, pp. 4012-4015, ISSN:0897-4756;
- Mada, Y.& Ione, N. (1986). p-n junction formation using laser induced donors in silicon, *Appl. Phys. Lett.*, Vol.48, pp.1205-1207, ISSN:0003-6951;
- Medvid', A. & Fedorenko, L. (1999). Generation of Donor Centers in p-InSb by Laser Radiation, *Materials Science Forum*, Vols. 297-298, pp. 311-314, ISSN:0255-5476;
- Medvid', A., Litovchenko, V.G., Korbutjak, D., Krilyk, S.G., Fedorenko, L.L.& Hatanaka ,Y. (2001). Influence of laser radiation on photoluminescence of CdTe, Influence of laser radiation on photoluminescence of CdTe *Radiation Measurements*, Vol. 33, pp. 725-72, ISSN:1350-4487;
- Medvid', A., (2002). Redistribution of the Point Defects in Crystalline Lattice of Semiconductor in Nonhomogeneous Temperature Field. *Defects and Diffusion Forum*, Vols. 210- 212 , pp. 89-101, ISSN:1012-0386;
- Medvid', A. & Lytvyn, P. (2004). Dynamics of Laser Ablation in SiC, *Materials Science Forum*, Vols. 457-460, pp. 411-414, ISSN:0255-5476;
- Medvid', Artur, Dmytruk, Igor, Onufrijevs, Pavels & Pundyk, Iryna. (2007). Quantum Confinement Effect in Nanohills Formed on a Surface of Ge by Laser Radiation. *Phys. Stat. Sol.(c)*, Vol.4, pp.3066-1069, ISSN: 1610-1634;
- Medvid' A., Onufrijevs, P., Dmytruk, I.& Pundyk, I. (2008). Properties of Nanostructure Formed on SiO₂/Si Interface by Laser Radiation, *Solid State Phenomena*, Vols. 131-133 pp. 559-562, ISSN: 1012-0394;
- Medvid', A., Mychko, A., Strilchyuk, O., Litovchenko, N., Naseka, Yu., Onufrijevs, P. & Pludonis, A. (2008).Exciton quantum confinement effect in nanostructures formed

- by laser radiation on the the surface of CdZnTe ternary compound, *Phys. Stat.Sol.(c)*, Vol.6, pp.209-212, ISSN: 1610-1634;
- Medvid' A., Onufrijevs, P., Lyutovich, K., Oehme, M., Kasper, E., Dmitruk, N., Kondratenko, O., I. Dmitruk & Pundyk, I. (2009). Self-assembly of nano-hills in $\text{Si}_x\text{Ge}_{1-x}/\text{Si}$ by laser radiation, *J. Nanoscience and Nanotechnol.* (in press), ISSN:1533-4880, ISSN:1533-4880;
- Medvid', A., Mychko, A., Gnatyuk, V. A., Levytskui, S. & Naseka, Y. Mechanism of nanostructure formation on a surface of CdZnTe crystal by laser irradiation. *J. Automation, Mobile Robotics & Intelligent Systems.*, Vol.3 pp.127-9. ISSN 1897-8649
- Mooney, P. M.; Jordan-Sweet J. L.; Ismail, K.; Chu, J. O.; Feenstra R. M. & LeGoues F. K. Relaxed $\text{Si}_{0.7}\text{Ge}_{0.3}$ buffer layers for high-mobility devices. (1995). *Appl. Phys. Lett.*, Vol.67, pp.2373-237, ISSN:0003-6951;
- Morales, A.M. & Lieber C.M. (1998). *Science*, Vol. 279, pp. 208-2, ISSN:0036-8075;
- Okhotin, A.S., Pushkarskii, A.S. & Gorbachev, V.V. (1972). *Thermophysical Properties of Semiconductors*, Atom, Moscow, (in Russian).
- Rebohle, L., von Borany, Frob, J.H. & Skorupa, W. (2000). *Appl.Phys.B: Lasers Opt.* Vol.B70 p. 131-13, ISSN: 0946-2171;
- Reno, J. & Jones, E. (1992). Determination of the dependence of the band-gap energy on composition for $\text{Cd}_{1-x}\text{Zn}_x\text{Te}$. *Phys. Rev. B*, Vol.45, pp.1440-1442, ISSN:1350-4487;
- Sun, K.W., Sue, S.H. & Liu, C.W. (2005). *Physica E*. Vol.28, pp.525-52, ISSN: 1386-9477;
- Talochkin, A. B., Teys, S. A. & Suprun, S. P. (2005). Resonance Raman scattering by optical phonons in unstrained germanium quantum dots, *Phys. Rev.* Vol.B 72, p.115416-11154, ISSN: 1098-0121;
- Vigil-Galán, O.; Arias-Carbajal, A.; Mendoza-Pérez, R.; Santana-Rodríguez, G.; Sastre-Hernández, J; Alonso, J C; Moreno-García, E.; Contreras-Puente, G. & Morales-Acevedo, A. (2005). Improving the efficiency of CdS/CdTe solar cells by varying the thiourea/ CdCl_2 ratio in the CdS chemical bath. *Semicond. Sci. Technol.* Vol.20, pp.819-822, ISSN 0268-1242;
- Von der Linde, D. & Fabricius, N. (1982). Observation of an electronic plasma in picosecond laser annealing of silicon. *Appl. Phys. Lett.*, Vol. 41, pp.991-993, ISSN: 0003-6951;
- Vorobyev, L.E., (1996). Semiconductor Parameters, In: Handbook Series, M. Levinshstein, S. Rumyantsev, M. Shur (Eds.), Vol.1, p. 232 ,World Scientific, ISBN: 978-981-02-2934-4, London;
- Werwa, E., Seraphin, A. A., Chiu, L. A., Zhou, C., & Kolenbrander K. D. (1996). Synthesis and processing of silicon nanocrystallites using a pulsed laser ablation supersonic expansion method. *Appl. Phys. Lett.* Vol.64, pp.1821-182, ISSN: 0003-6951;
- Wu, X. L.; Gao, T.; Bao, X. M; Yan, F.; Jiang, S. S. & Feng, D. (1997). Annealing temperature dependence of Raman scattering in Ge^+ -implanted SiO_2 films. *J. Appl. Phys.* Vol. 82 pp. 2704, ISSN:0003-6951;
- Yoshida, T., Yamada, Y. & Orii, T. (1998). Electroluminescence of silicon nanocrystallites prepared by pulsed laser ablation in reduced pressure inert gas. *J. Appl. Phys.* Vol. 83(10), pp.5427-32, ISSN: 0021-8979;
- Xia, Y. & Yang, Y. (2003). Chemistry and physics of nanowires. *Advanced Materials*, Vol. 15, pp.351-353, ISSN: 0935-9648.



Nanowires Science and Technology

Edited by Nicoleta Lupu

ISBN 978-953-7619-89-3

Hard cover, 402 pages

Publisher InTech

Published online 01, February, 2010

Published in print edition February, 2010

This book describes nanowires fabrication and their potential applications, both as standing alone or complementing carbon nanotubes and polymers. Understanding the design and working principles of nanowires described here, requires a multidisciplinary background of physics, chemistry, materials science, electrical and optoelectronics engineering, bioengineering, etc. This book is organized in eighteen chapters. In the first chapters, some considerations concerning the preparation of metallic and semiconductor nanowires are presented. Then, combinations of nanowires and carbon nanotubes are described and their properties connected with possible applications. After that, some polymer nanowires single or complementing metallic nanowires are reported. A new family of nanowires, the photoferroelectric ones, is presented in connection with their possible applications in non-volatile memory devices. Finally, some applications of nanowires in Magnetic Resonance Imaging, photoluminescence, light sensing and field-effect transistors are described. The book offers new insights, solutions and ideas for the design of efficient nanowires and applications. While not pretending to be comprehensive, its wide coverage might be appropriate not only for researchers but also for experienced technical professionals.

How to reference

In order to correctly reference this scholarly work, feel free to copy and paste the following:

Artur Medvid' (2010). Nano-Cones Formed on a Surface of Semiconductors by Laser Radiation: Technology, Model and Properties, Nanowires Science and Technology, Nicoleta Lupu (Ed.), ISBN: 978-953-7619-89-3, InTech, Available from: <http://www.intechopen.com/books/nanowires-science-and-technology/nano-cones-formed-on-a-surface-of-semiconductors-by-laser-radiation-technology-model-and-properties>

INTECH
open science | open minds

InTech Europe

University Campus STeP Ri
Slavka Krautzeka 83/A
51000 Rijeka, Croatia
Phone: +385 (51) 770 447
Fax: +385 (51) 686 166
www.intechopen.com

InTech China

Unit 405, Office Block, Hotel Equatorial Shanghai
No.65, Yan An Road (West), Shanghai, 200040, China
中国上海市延安西路65号上海国际贵都大饭店办公楼405单元
Phone: +86-21-62489820
Fax: +86-21-62489821

© 2010 The Author(s). Licensee IntechOpen. This chapter is distributed under the terms of the [Creative Commons Attribution-NonCommercial-ShareAlike-3.0 License](https://creativecommons.org/licenses/by-nc-sa/3.0/), which permits use, distribution and reproduction for non-commercial purposes, provided the original is properly cited and derivative works building on this content are distributed under the same license.

IntechOpen

IntechOpen